

Hierarchical Finite Element Simulation of Perforated Plates with Arbitrary Hole Geometries

P. Råback*, A. Pursula*, V. Junttila** and T. Veijola**

CSC – Scientific Computing, P.O. Box 405, FIN-02101 Espoo, Finland,
peter.raback@csc.fi and antti.pursula@csc.fi
Helsinki University of Technology, Finland
virpi.junttila@hut.fi and timo.veijola@hut.fi

ABSTRACT

A two-level hierarchical simulation strategy for gas damped microdevices including perforated structures is presented. The first level of hierarchy consists of finding the flow resistance of a single hole using 3D numerical simulation. The second level of hierarchy is the coupled reduced dimensional simulation of the device including mechanical, electrostatic and fluidic phenomena. The method can be used to model time-dependent problems including large displacements. The scheme is applied to the simulation of a membrane with hexagonal perforation in the cases of transient pull-in and damped large-amplitude oscillation.

Keywords: perforated, hierarchical model, finite element method

1 INTRODUCTION

The squeezed-film-damping of micro-electro-mechanical devices may be reduced significantly by creating a number of small holes into the structure. Unfortunately, in numerical simulations, it is possible to consider only a few holes in detail, since a larger system makes the computational cost too high. A more feasible approach is to homogenize the contribution of the holes over the whole domain. This approach may be used to account for the effects caused by perforation in microfluidistics [1]–[3], in electrostatics as well as in elasticity [4].

In this paper we follow a hierarchical two-level simulation strategy. We take a unit cell including one hole and compute the flow resistance as a function of the air gap height. From this calculation, the homogenized flow resistance is extracted, and used in the coupled reduced dimensional analysis including fluidic, elastic and electrostatic forces.

2 THEORY

2.1 Level 1: Homogenization of Holes

The flow resistance of a single hole can be determined by simulating numerically the gas flow through the hole. The geometry for the simulation should include a unit cell of the structure consisting of the perforated body, air gap and a region of space above the hole. The geometry

should extend on the intermediate area between adjacent holes up to the symmetry plane. The void region above the hole should be large enough to avoid any artificial effects due to the boundaries of the computational domain. It suffices to use a velocity boundary condition for the gas instead of simulating the movement of the elastic structure.

From the flow field the force F acting on the elastic plate may be computed. There is a monotonic dependence between the force and the velocity of the moving structure, v . The dependence is linear, if the equation describing the fluid flow is linear. Further, if the compressibility of the gas may be neglected, no phase shift between wake velocity and response force can appear, and the ratio between these quantities is a single real value.

The ratio F/v describes the flow resistance in the unit cell for each height of the air gap. The flow resistance may be averaged with respect to the area of the unit cell, A_h , resulting in the specific acoustic impedance [5],

$$z_h = \frac{F}{vA_h}. \quad (1)$$

The simulations should be performed on a number of different air gaps. The horizontal flow into the hole is affected by the height of the air gap, d , whereas the flow resistance through the hole remains approximately unchanged. The results may be used to define a specific acoustic impedance that is a function of the air gap height, $z_h = z_h(d)$.

For the linearity of the Navier-Stokes equations, we can argue that the mass term of the equations is small since the Reynolds number of the problem is small

$$Re = \frac{\rho UL}{\eta} \approx 10^{-3}, \quad (2)$$

where ρ and η are, respectively, the density and the viscosity of the gas and U and L are, respectively, the velocity and length scales of the problem.

The low value of the Reynolds number implies that the convection term of the Navier-Stokes equations can be neglected. Also, when the compressibility of the gas is negligible, the flow is not time-dependent if the boundary conditions do not depend on time. Thus, the fluid

flow is governed by the stationary Stokes equation

$$-\nabla \cdot (2\eta \bar{\epsilon}) + \nabla p = \rho \vec{f}, \quad (3)$$

where p is the pressure, $\rho \vec{f}$ is a body force and $\bar{\epsilon}$ is the linearized strain tensor. For incompressible gases, the condition $\nabla \cdot \vec{u}$ for the gas velocity \vec{u} is also required.

The gas flow can be assumed incompressible since the gas velocity stays well below the speed of sound in operating conditions, which implies very low Mach number, and thus incompressible flow [6]. Certainly, the nature of the gas in this respect depends on the frequency of the membrane's oscillations. The conclusions made above are valid for microsystems typically when the oscillations are below radio frequencies.

Also the temperature changes and viscous pressure variations can be studied by non-dimensional analysis to determine if they have an effect on the gas density [7]. All in all, the compressibility issue is difficult to answer without numerical tests which should preferably be performed.

Also, in order to the Stokes (or Navier-Stokes) equation to be valid, the flow has to be on the continuum regime which means that the dimensions of the geometry may not be arbitrarily small. The importance of the gas rarefaction effect can be stated with the Knudsen number

$$Kn = \frac{\mathcal{L}}{L}, \quad (4)$$

where \mathcal{L} is the mean free path of gas molecules. In normal conditions, the mean free path for air is a little below 100 nm so that geometries with air gaps down to 1 μm are suitable for continuum approach when slip boundary conditions are used [7]. The mean free path, however, is inversely proportional to the ambient pressure, and thus the applicability of the continuum approach is further limited in conditions where the ambient pressure is low.

2.2 Level 2: Coupled Simulation

The second hierarchy level consists of solving a coupled system of equations describing the fluidic, electrostatic and elastic phenomena. In this paper the thickness of the structure and the air gap are assumed to be small compared to the other dimensions. This makes it possible to describe the behavior of the structure with reduced dimensional equations. Therefore the structure is modeled with a 2D plate equation, the electrostatics with 1D potential equation and the fluid with a 2D Reynolds equation.

The transient Reynolds equation for large displacements is

$$\nabla \cdot \left(\frac{pd^3}{12\eta} \nabla p \right) = \frac{\partial(pd)}{\partial t}. \quad (5)$$

where p is the absolute pressure and d is the air gap height.

For perforated plates the Reynolds equation must be modified so that the additional term due to the holes is accounted for. The pressure drop over the hole is obviously $\Delta p = p - P$, where P is the reference pressure. Assuming small pressure deviations the equation can be written [3]

$$\nabla \cdot \left(\frac{pd^3}{12\eta} \nabla p \right) - \frac{1}{z_h} p(p - P) = \frac{\partial(pd)}{\partial t}, \quad (6)$$

where z_h is the specific acoustic impedance obtained from 3D simulations.

When the size of the holes diminishes the acoustic impedance approaches infinity and therefore the original Reynolds equation is restored. On the other hand, when the acoustic impedance is small the equation simplifies to

$$P - p = z_h \frac{\partial d}{\partial t}. \quad (7)$$

Comparing this to Eq. 1 and noting that the pressure difference is just the net force per area we may conclude the equation returns the correct pressure at the limit. Thus, the modified Reynolds equation models the extreme cases accurately. The intermediate region where the relative importance of vertical and horizontal flow is equally important may be more susceptible to errors.

For electrostatics we use the fact that for nearly perpendicular plates the magnitude of the electric field may be approximated by $E = \Phi/d$, where Φ is the potential difference. The electric energy density is

$$e = \frac{1}{2} \epsilon E^2 d = \frac{\epsilon \Phi^2}{2d}, \quad (8)$$

from which the force density is obtained by derivation,

$$f = \frac{\partial e}{\partial d} = -\frac{\epsilon \Phi^2}{2d^2}. \quad (9)$$

For the elastic membrane we use a Kirchhoff type of linear plate model,

$$\rho h \frac{\partial^2 w}{\partial t^2} + K \Delta \Delta w - T \Delta w = p + f, \quad (10)$$

where $K = Et^3/[12(1 - \nu^2)]$ is the bending stiffness, E is Young's modulus, ν Poisson ratio, and T the surface tension. A linear model is sufficient if the maximum displacement w is significantly smaller than the thickness of the plate h . If the plate is pre-stressed the region of validity further increases.

The full system includes Equations 9, 10 and 6. The dependence between the height of the air gap d and displacement w is needed to close the system. For aligned plates the dependence is simple, $d = D - w$, where D is the air gap height at rest. The solution for each time-step is found by a loosely coupled iteration scheme where the equations are solved consecutively until the convergence criteria are met.

3 RESULTS

Numerical simulations with the two-level strategy were performed for a resonating square membrane with an opposing backplate with hexagonal perforation holes.

The size chosen for the membrane was $1\text{ mm} \times 1\text{ mm} \times 1\text{ }\mu\text{m}$. The elastic parameters used were $E=160\text{ GPa}$, $\nu=0.30$, $\rho=2300\text{ kg/m}^3$, and $T=2\text{ MPa/m}$. The rigid backplate was $10\text{ }\mu\text{m}$ thick and filled with hexagonal holes with a diameter of $8\text{ }\mu\text{m}$ and area fraction of $4/9$. The viscosity of the air was $\eta=20.8\text{e-6 Pa s}$ and the air gap height at rest was $1\text{ }\mu\text{m}$.

The computations were performed with Elmer finite element software [8] that includes many tailored models for simulating micro-electro-mechanical devices.

3.1 Analysis of Hexagonal Holes in 3D

The simulation geometry for resistance extraction is pictured in Fig 1. The Stokes equation was given a constant velocity boundary condition on the lower wall and the upper boundary was left open. The open sides were modeled with symmetry conditions and no-slip conditions were used on other walls. The simulations were performed with various air gaps and the net force acting on the lower boundary was computed. An accurate analytical model for the specific acoustic impedance was obtained by a least-square fit of the function

$$z_h(d) = (d_0/d)^n + z_0, \quad (11)$$

where n is 2.475, d_0 is $10.75\text{ }\mu\text{m}$ and z_0 is $323.6\text{ kg/m}^2\text{s}$. The results with the fitted function are pictured in Fig. 2.

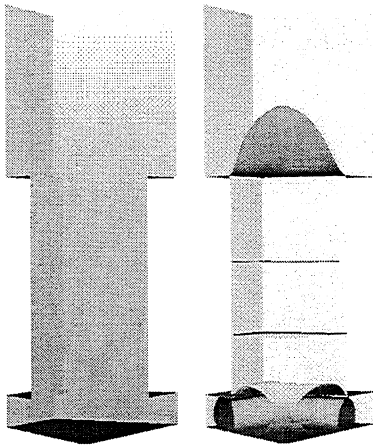


Figure 1: The quadrant of one hexagonal hole (left) with pressure isobars (right).

Also, the applicability of the linearity and incompressibility assumptions were studied. Following the procedure in [7] the relative importance of the viscous pressure changes as well as assumed temperature changes were studied and their effect on the gas density was

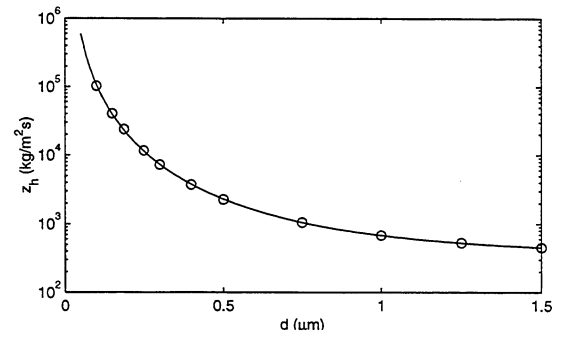


Figure 2: Numerical results (circles) and the fitted function for the specific acoustic impedance as a function of air gap height.

found to be negligible. The complimentary numerical tests showed that the incompressible Stokes equation is sufficient approximately down to gaps of $0.2\text{ }\mu\text{m}$. Thus, linear dependence between velocity and net force without phase change was assumed.

3.2 Transient Membrane Simulations

As a second step, transient simulations for the resonating membrane were performed. Here, the analytical fit for the specific acoustic impedance z_h was used. The dynamical pull-in phenomenon and the damping of a pressure pulse initiated oscillation were studied.

The dynamical pull-in phenomenon occurs when the bias voltage between the membrane and the backplate is larger than the critical pull-in voltage and the membrane is initially at rest. Here a voltage difference of $\Phi=2\text{ V}$ was chosen. The results with two different reference pressures were compared to the undamped case. The minimum air gap heights with time for the three cases are depicted in Fig. 3. For each case the starting phase is similar as the inertial forces dominate. The undamped case is in an accelerating motion until the pull-in occurs, whereas in the damped cases the velocity reaches a value where the attracting force and the fluidic resistance are in balance.

The maximum pressure difference over the membrane in the two damped cases is shown in Fig. 4. The pressure increases dramatically when contact is approaching. Strictly speaking, in the present model contact cannot occur since the pressure approaches infinity as the membrane approaches the backplate. The time of contact could be modeled if slip conditions for the flow were used.

The gas damping effect is clearly demonstrated in the pressure pulse initiated oscillation of the membrane. The wake for the membrane was a pressure pulse of 10 Pa applied for $10\text{ }\mu\text{s}$ duration. Simulations were carried out for an undamped system and damped systems in the ambient pressures of 1 and 0.1 atmospheres. As

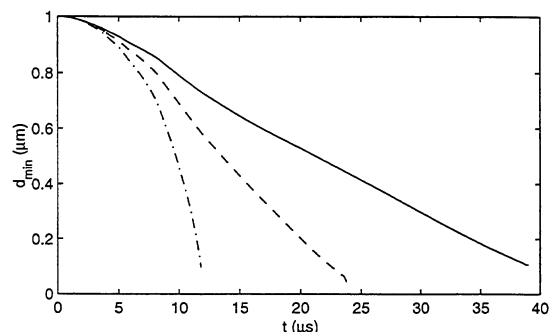


Figure 3: The minimum air gap height as function of time for undamped (dash-dot line) and damped cases with $P=1.0$ atm and $P=0.5$ atm (dashed line).

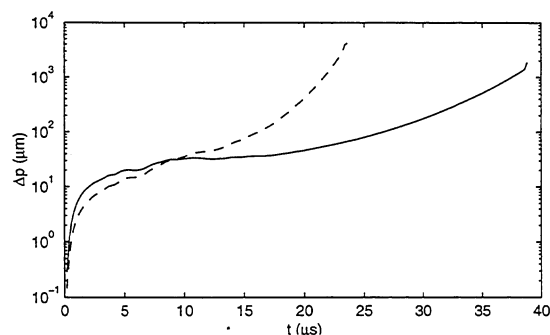


Figure 4: The maximum pressure difference with time for damped cases with $P = 1.0$ atm and $P=0.5$ atm (dashed line).

seen in Fig. 5, the movement of the membrane in the latter cases is gradually damped.

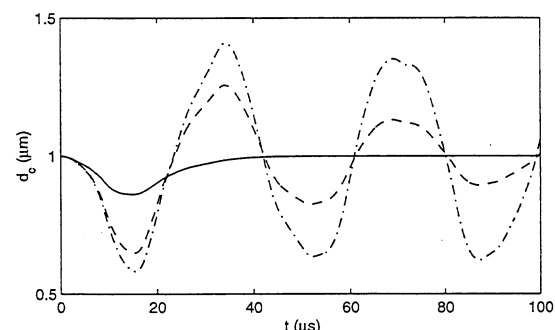


Figure 5: The air gap height at center as function of time for undamped (dash-dot line) and damped cases with $P=1.0$ atm and $P=0.1$ atm (dashed line).

4 CONCLUSIONS

We have presented a hierarchical simulation method for an elastic membrane under electrostatic and fluidic

forces, in which the effect of arbitrary shaped perforation holes can be taken into account. The method can be used in time-dependent simulations and is not limited to small displacements. The approach may be applied to a variety of micro-electro-mechanical systems, such as planar accelerometers, microphones, pressure sensors and resonators.

The simple homogenization of the holes is possible only if the underlying phenomena are linear in nature. Therefore the use of Stokes equation in the flow simulations is not only a more economical alternative to the Navier-Stokes equation but also a prerequisite for a successful homogenization.

The validity of the 3D flow simulations is essential to the accuracy of the results. The no-slip boundary condition is not realistic in small dimensions. For better accuracy slip conditions should be adopted.

Basically, the hierarchical strategy is not dependent on the particular method used to determine the flow resistance. In principle, the method could be used also with Monte Carlo simulations of rarefied gases, for example. As long as the specific acoustic impedance is found out, the second level of hierarchy can be applied.

The perforation effects have been accounted only for the gas flow where the holes dominate the behavior. The perforation also affects the electrostatic forces and sometimes also the elasticity. Here the effect is on the same order of magnitude as the fraction of the perforation holes.

In this paper we have only dealt with planar structures where the reduced dimensional equations may be used. The hierarchical approach is not, however, limited to the reduced equations. We have, for example, used homogenization of flow resistance together with 3D elasticity equations.

REFERENCES

- [1] Y.-J. Yang and C.-J. Yu, Proceedings of the 5th International Conference on Modeling and Simulation of Microsystems, 178–181, 2002.
- [2] M. G. da Silva, M. Deshpande and K. Greiner, J. R. Gilbert, Proceedings of Transducers'99, 2, 1148–1151, 1999.
- [3] T. Veijola and T. Mattila, Proceedings of Transducers'01, 2, 1506–1509, 2001.
- [4] M. Pedersen, W. Olthuis and P. Bergveld, Sensors and Actuators A, 54, 499–504, 1999.
- [5] D. T. Blackstock, "Fundamentals of Physical Acoustics," John Wiley & Sons, 2000.
- [6] F. M. White, "Fluid Mechanics," McGraw-Hill, 1994.
- [7] M. Gad-el-Hak, J. Fluids Eng., 121, 5–33, 1999.
- [8] Elmer software, <http://www.csc.fi/elmer>.